Article

Not peer-reviewed version

Dysregulated DNA Methylation in Retinal Pigment Epithelium During the Early Stage of Stargardt Disease

Arpita Dave *, Anela Tosevska, Marco Morselli, Emily Tom, Matteo Pellegrini, Dorota Skowronska-Krawczyk *, Roxana A Radu *

Posted Date: 2 September 2025

doi: 10.20944/preprints202509.0141.v1

Keywords: recessive Stargardt disease; retinal pigment epithelium; DNA methylation; methyl-CpG-binding protein 2; reduced representation bisulfite sequencing

 doi:10.20944/preprints202509.0141.v1

Article

Dysregulated DNA Methylation in Retinal Pigment Epithelium During the Early Stage of Stargardt Disease

Arpita Dave [1,*], Anela Tosevska [2,3], Marco Morselli [2], Emily Tom [4], Matteo Pellegrini [2], Dorota Skowronska-Krawczyk [4,*] and Roxana A. Radu [1,*]

[1] UCLA Jules Stein Eye Institute and Department of Ophthalmology, David Geffen School of Medicine, UCLA, Los Angeles, USA
[2] Department of Molecular, Cell, and Developmental Biology, UCLA, USA
[3] Medical University of Vienna, Division of Rheumatology, Department of Internal Medicine 3, Vienna, Austria
[4] Robert M. Brunson Center for Translational Vision Research, Department of Physiology and Biophysics, Department of Ophthalmology and Visual Sciences, School of Medicine, UC Irvine, USA
* Correspondence: arpita2269@g.ucla.edu (A.D.); dorotask@hs.uci.edu (D.S.-K.); radu@jsei.ucla.edu (R.A.R.)

Abstract

Stargardt disease (STGD1), the most common inherited juvenile macular degeneration, is caused by biallelic mutations in the ABCA4 gene. Currently, there is no approved treatment. In this study, we investigated early-stage epigenomic changes in the retinal pigment epithelium (RPE) of *Abca4*$^{-/-}$ mice, a well-established model of STGD1. Reduced representation bisulfite sequencing (RRBS) revealed hypermethylation of gene regions associated with disease-related pathways, implicating methyl-CpG-binding protein 2 (MeCP2) and RE1-silencing transcription factor (REST) as potential regulators. Notably, DNA methylation of a subset of genes preceded their transcriptional change and disease phenotypes in *Abca4*$^{-/-}$ RPE. Together with the detected age-dependent increase in MeCP2 levels in *Abca4*$^{-/-}$ RPE, these findings suggest that early DNA methylation changes may contribute to RPE dysfunction and eventual cell loss in STGD1.

Keywords: recessive Stargardt disease; retinal pigment epithelium; DNA methylation; methyl-CpG-binding protein 2; reduced representation bisulfite sequencing

1. Introduction

Loss of retinal pigment epithelial cell (RPE) structural and functional integrity causes death of photoreceptors, leading to macular dystrophy in the recessive Stargardt disease (STGD1) [1–4]. Mutations in the ATP-binding cassette transporter (*ABCA4*) gene are responsible for STGD1, a juvenile blinding disease [5,6]. Currently, there are *no* efficacious treatments for STGD1. While ABCA4 is well known for its role in photoreceptors, it is also expressed and functions in the membranes of RPE cells [7–13]. Studies in RPE cells derived from patients with *ABCA4* mutations and *Abca4* knock-out mice display disease-associated phenotypes, such as increasing accumulation of vitamin A dimers (bisretinoids), complement system dysregulation, endolysosomal and mitochondrial dysfunctions [14–18], all of which are mediated by differential gene expressions.

DNA methylation, an epigenetic modification that involves adding methyl groups to cytosine residues of DNA in CpG (cytosine-phosphate-guanine) sites, is a dynamic process for the regulation of gene expression. The majority of CpGs are found within CpG islands, the DNA regions with GC content greater than 50% and are associated with 70% of annotated gene promoters [19]. DNA methylation was first identified as the DNA modification involved in gene repression [20]; however, more recent studies demonstrate that DNA methylation acts as context-dependent regulation,

 doi:10.20944/preprints202509.0141.v1

functioning both as a gene repressor and an activator based on its location in the gene [21,22]. Regulation of gene transcription by DNA methylation is mediated by proteins that recognize CpG duplexes involving: (1) DNA methyl region-binding proteins, (2) DNA methylases or methyltransferases, and (3) DNA demethylases [23].

Methyl-CpG-binding 2 (MeCP2), a protein that binds methylated CpGs [24], has been extensively studied in the central nervous system (CNS) due to its mutations linked to Rett syndrome, a neurodevelopmental disorder [25]. In CNS cells, MeCP2 deficiency and overexpression have been reported to induce a spectrum of dysfunctions through the role of MeCP2 in transcription activation, repression, chromatin remodeling, and RNA splicing [26–32]. Embryologically, the CNS, retina, and RPE all originate from the neuroectoderm [33], sharing common pathways for their development. In the eye, MeCP2 expression in photoreceptors begins during the postnatal period (P0–P16), whereas in the RPE, it is detectable as early as the embryonic stage (E12) and persists throughout life [34]. On a functional level, MeCP2 binds to the TGF-β gene promoter in RPE cells [35] and regulates epithelial-mesenchymal transition (EMT) [36,37], a key pathogenic mechanism linked to age-related macular degeneration (AMD) [38]. Additionally, reduced MeCP2 levels impair RPE ciliogenesis [39], a process essential for RPE development and stress response. Disruption of ciliogenesis was linked to retinal degeneration [40]. Despite these findings, the potential role of MeCP2 in both the neural retina and RPE in the context of disease remains unknown.

To test the hypothesis that early DNA methylation changes contribute to RPE dysfunction in STGD1 through MeCP2-mediated mechanisms, we performed Reduced Representation Bisulfite Sequencing (RRBS), transcriptomic analyses, and MeCP2 protein level assessment on RPE/eyecups from *Abca4*$^{-/-}$ and wild-type mice. Our results suggest that DNA methylation, together with the co-transcriptional regulators MeCP2 and REST, contributes to progressive dysregulation of the transcriptomic makeup of RPE cells and age-dependent molecular modifications in *Abca4*$^{-/-}$ mice. These findings provide insight into how altered DNA methylation patterns may contribute to the disease progression in STGD1, informing us on the underlying mechanistic pathways of cell death and guiding the development of novel therapeutic strategies.

2. Results

2.1. RRBS Identified Altered DNA Methylation in RPE of 1-Month Abca4$^{-/-}$ *Mice*

Abca4$^{-/-}$ mice recapitulate key features of STGD1 phenotype, exhibiting detectable levels of bisretinoid-autofluorescence in the RPE as early as 1 month of age [18,41]. By 6 months, RPE dysfunction is evident, and by 9 to 12 months, loss of RPE and photoreceptor cells is reported [11,41,42]. To investigate early DNA methylation changes, we analyzed differentially methylated CpGs (DMC) in RPE tissue from age-matched 1- and 3-month-old wild-type and *Abca4*$^{-/-}$ mice (Figure 1A). Genome-wide profiling of methylated CpG sites revealed the following distribution: 0.39% in CpG islands, 3.24% in promoters, 3.24% in first exons, 3.24% in proximal regulatory region (1-5 kb upstream of transcriptional start site), 2.17% in 5' untranslated regions (UTR), 15.93% in introns, 19.18% in exons, 17.47% in intron-exon and 17.45% at exon-intron boundaries, 12.03% in coding sequence, and 5.64% in other regions (including lncRNA, intergenic, CpG shores, CpG shelves, and enhancers) captured by RRBS (Figure 1B), consistent with distribution described in other tissues [43].

 doi:10.20944/preprints202509.0141.v1

Figure 1

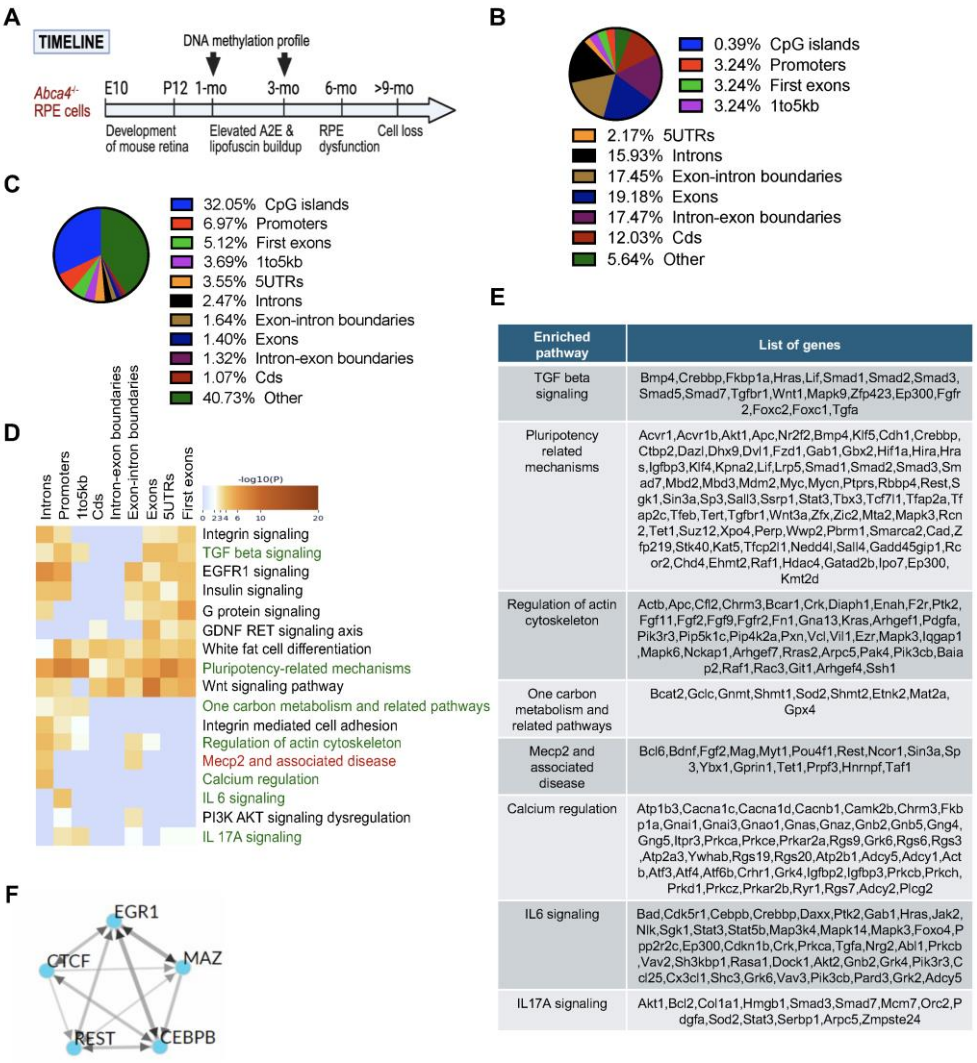

E

Enriched pathway	List of genes
TGF beta signaling	Bmp4,Crebbp,Fkbp1a,Hras,Lif,Smad1,Smad2,Smad3,Smad5,Smad7,Tgfbr1,Wnt1,Mapk9,Zfp423,Ep300,Fgfr2,Foxc2,Foxc1,Tgfa
Pluripotency related mechanisms	Acvr1,Acvr1b,Akt1,Apc,Nr2f2,Bmp4,Klf5,Cdh1,Crebbp,Ctbp2,Dazl,Dhx9,Dvl1,Fzd1,Gab1,Gbx2,Hif1a,Hira,Hras,Igfbp3,Klf4,Kpna2,Lif,Lrp5,Smad1,Smad2,Smad3,Smad7,Mbd2,Mbd3,Mdm2,Myc,Mycn,Ptprs,Rbbp4,Rest,Sgk1,Sin3a,Sp3,Sall3,Ssrp1,Stat3,Tbx3,Tcf7l1,Tfap2a,Tfap2c,Tfeb,Tert,Tgfbr1,Wnt3a,Zfx,Zic2,Mta2,Mapk3,Rcn2,Tet1,Suz12,Xpo4,Perp,Wwp2,Pbrm1,Smarca2,Cad,Zfp219,Stk40,Kat5,Tfcp2l1,Nedd4l,Sall4,Gadd45gip1,Ror2,Chd4,Ehmt2,Raf1,Hdac4,Gatad2b,Ipo7,Ep300,Kmt2d
Regulation of actin cytoskeleton	Actb,Apc,Cfl2,Chrm3,Bcar1,Crk,Diaph1,Enah,F2r,Ptk2,Fgf11,Fgf2,Fgf9,Fgfr2,Fn1,Gna13,Kras,Arhgef1,Pdgfa,Pik3r3,Pip5k1c,Pip4k2a,Pxn,Vcl,Vil1,Ezr,Mapk3,Iqgap1,Mapk6,Nckap1,Arhgef7,Rras2,Arpc5,Pak4,Pik3cb,Baiap2,Raf1,Rac3,Git1,Arhgef4,Ssh1
One carbon metabolism and related pathways	Bcat2,Gclc,Gnmt,Shmt1,Sod2,Shmt2,Etnk2,Mat2a,Gpx4
Mecp2 and associated disease	Bcl6,Bdnf,Fgf2,Mag,Myt1,Pou4f1,Rest,Ncor1,Sin3a,Sp3,Ybx1,Gprin1,Tet1,Prpf3,Hnrnpf,Taf1
Calcium regulation	Atp1b3,Cacna1c,Cacna1d,Cacnb1,Camk2b,Chrm3,Fkbp1a,Gnai1,Gnai3,Gnao1,Gnas,Gnaz,Gnb2,Gnb5,Gng4,Gng5,Itpr3,Prkca,Prkce,Prkar2a,Rgs9,Grk6,Rgs6,Rgs3,Atp2a3,Ywhab,Rgs19,Rgs20,Atp2b1,Adcy5,Adcy1,Actb,Atf3,Atf4,Atf6b,Crhr1,Grk4,Igfbp2,Igfbp3,Prkcb,Prkch,Prkd1,Prkcz,Prkar2b,Ryr1,Rgs7,Adcy2,Plcg2
IL6 signaling	Bad,Cdk5r1,Cebpb,Crebbp,Daxx,Ptk2,Gab1,Hras,Jak2,Nlk,Sgk1,Stat3,Stat5b,Map3k4,Mapk14,Mapk3,Foxo4,Ppp2r2c,Ep300,Cdkn1b,Crk,Prkca,Tgfa,Nrg2,Abl1,Prkcb,Vav2,Sh3kbp1,Rasa1,Dock1,Akt2,Gnb2,Grk4,Pik3r3,Ccl25,Cx3cl1,Shc3,Grk6,Vav3,Pik3cb,Pard3,Grk2,Adcy5
IL17A signaling	Akt1,Bcl2,Col1a1,Hmgb1,Smad3,Smad7,Mcm7,Orc2,Pdgfa,Sod2,Stat3,Serbp1,Arpc5,Zmpste24

Figure 1. Hypermethylated genomic DNA in pigmented 1-mo *Abca4*$^{-/-}$ mice RPE. (A) Timeline of retinal development and STGD1 disease phenotypes in *Abca4*$^{-/-}$ mice. Retina development of mice occurs during embryonic (E) day 10 to postnatal (P) day 12 [59]. Within the first month, bisretinoids (A2E) and lipofuscin-autofluorescence buildup are initiated in the RPE of mice lacking ABCA4, leading to dysfunction and death of RPE from age >6-mo. (B) Genomic distribution of methylated CpG sites covered by RRBS. The pie chart displays the distribution of CpG sites, classified by genomic feature from RRBS data generated in 1-month-old and 3-month-old *Abca4*$^{-/-}$ and wild-type mice (129/Sv and BALB/c strains). Genomic coverage in RRBS was assessed at single-nucleotide resolution, specifically at CpG dinucleotides. The genomic distribution of methylated CpG sites across all samples revealed that 0.39% were located in CpG islands, 3.24% in promoters, 3.24% in first exons, and the remainder across various genomic regions. (C) Genomic distribution of DMCs in *Abca4*$^{-/-}$ versus wild-type RPE. (D) Gene ontology and pathway enrichment analysis of hypermethylated DMCs. (biological 3 samples, one RPE/EC per sample). (E) Hypermethylated gene list in key regulatory pathways affected in *Abca4*$^{-/-}$ mice RPE. (F) Transcription factors associated with hypermethylated DMC-promoters in *Abca4*$^{-/-}$ mice.

Differential analysis of RPE from 1-month-old *Abca4*$^{-/-}$ mice, demonstrated that DMCs were predominantly enriched in proximal regulatory elements such as CpG islands (32%), promoters (6.97%), first exons (5.12%), and 1 to 5 kb gene regions (3.69%) (Figure 1C). These findings suggest

 doi:10.20944/preprints202509.0141.v1

that transcription activation, rather than other stages of gene expression regulation, may be the primary mechanism affected. Enrichment analysis of hypermethylated DMC-associated genes identified significant involvement of pathways implicated in RPE function and degeneration. Markedly, enriched pathways included MeCP2 and its related disorders (p-value= $8.59x10^{-5}$), TGF-β signaling (p-value= $2.64x10^{-5}$), pluripotency regulation (p-value= $4.10x10^{-12}$), actin cytoskeleton dynamics (p-value= $5.11x10^{-7}$), calcium signaling (p-value= $2.07x10^{-5}$), one-carbon metabolism (p-value= $7.42x10^{-4}$), IL-6 signaling (p-value= $5.08x10^{-5}$), and IL-17A signaling (p-value= $4.01x10^{-4}$) (Figure 1D-E), all previously linked to neurodegenerative diseases and dysfunction of RPE in AMD [44–49].

2.2. Transcription Factors Associated with Hypermethylated DMC-Promoters in Abca4$^{-/-}$ Mice RPE at 1-Month of Age

To identify potential upstream regulators affected by an increased DNA methylation in Abca4$^{-/-}$ RPE, we performed ChEA3 transcription factor binding site enrichment analysis [50] using promoter sequences corresponding to significantly hypermethylated DMCs regions in 1-month-old Abca4$^{-/-}$ animals. This analysis revealed significant enrichment of binding sites for EGR1, CTCF, REST, CEBPB, and MAZ (Figure 1F). These transcription regulators are known to function as site-specific regulators (EGR1 and MAZ) [51,52], transcription co-activators (CEBPB) [53], and chromatin organizers (CTCF and REST) [54,55]. Notably, REST has been previously shown to interact with MeCP2 and to be implicated in epigenetic regulation in neurodegeneration [56,57].

Figure 2

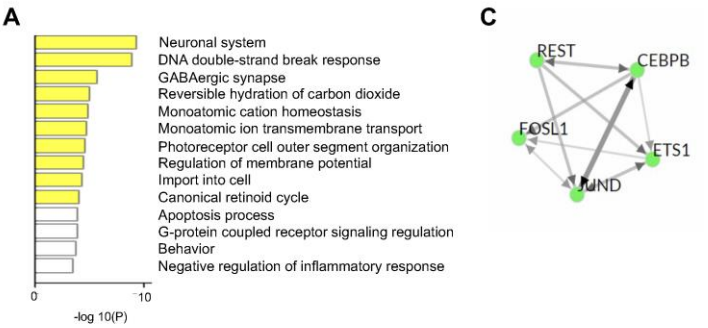

B

Enriched pathway	List of genes
DNA double-strand break response	Brca1,Kpna2,H4c8,H4c3,H4c4,H4c11,H4c18,H2bc15,H4c16,H4c1, H4c17
Monoatomic cation homeostasis	Agtr2,Alas2,Calb1,Calb2,Car2,Car4,Casq2,Ccr2,Cnga1,Drd4,Mt3,Ppt 1,Slc8a1,Cacna1f,Fxyd1,Slc12a5,Ccdc115,Npy,Scgn
Regulation of membrane potential	Chrna6,Casq2,Cnga1,Drd4,Fgf12,Gabra1,Gabrg2,Gabrr1,Gjd2,Hcn1, Htr3a,Slc6a4,Myoc,Slc8a1,Fxyd1,Slc17a7,Rims2,Kcnv2,Slc1a7
Apoptosis process	Igf1,Pde6b,Grk1,Ins2,Esrrb,Mt3,Fabp5,Slc1a2,Upk3b
Negative regulation of inflammatory response	Igf1,Il12b,Ins2,Isl1,Tnfaip3,Tnfaip6,Aoah,Npy,Clec12

Figure 2. Downregulated gene expression in pigmented 1-mo *Abca4*$^{-/-}$ mice RPE. (A) Gene ontology and pathway enrichment analysis of RNA sequencing data. Colors indicate varying levels of statistical significance. (n= 3 biological replicates). (B) Downregulated genes list of key regulatory pathways affected in *Abca4*$^{-/-}$ mice RPE. (C) Transcription factors associated with downregulated DEGs in *Abca4*$^{-/-}$ mice.

2.3. RNA-seq Analysis Identified Transcriptional Changes in RPE from 1-Month-Old Abca4$^{-/-}$ Mice Compared to Age-Matched Wild-Type Controls

To assess the extent to which hypermethylation of proximal regulatory regions correlates with transcriptional downregulation in the RPE of 1-month-old *Abca4*$^{-/-}$ mice, we analyzed a publicly available RNA-seq dataset (GSE63772). Differentially expressed genes (DEGs) were identified using

 doi:10.20944/preprints202509.0141.v1

a threshold of fold change >1 and adjusted *p*-value < 0.05. Gene ontology analysis revealed significant downregulation of genes involved in DNA repair (*p*-value= $3.6x10^{-6}$), monoatomic cation homeostasis (*p*-value= $4.3x10^{-5}$), regulation of membrane potential (*p*-value= $3.2x10^{-5}$), apoptotic processes (*p*-value= $1.5x10^{-4}$), and negative regulation of inflammatory response (*p*-value= $3.7x10^{-4}$) (Figure 2A,B).

ChEA3 analysis of regulatory elements of downregulated genes identified FOSL1, JUND, ETS1, CEBPB, and REST as the top five transcription factors binding motifs associated with these changes (Figure 2C). Remarkably, analysis of hypermethylated regions at the same stage of disease revealed a REST binding site, a key co-factor of MeCP2, underscoring the critical role of MeCP2-REST complex in driving early transcriptional reprogramming in STGD1 RPE.

2.4. DNA Methylation Enriched Pathways in 3-Month-Old Abca4$^{-/-}$ Mice RPE Cells

Figure 3

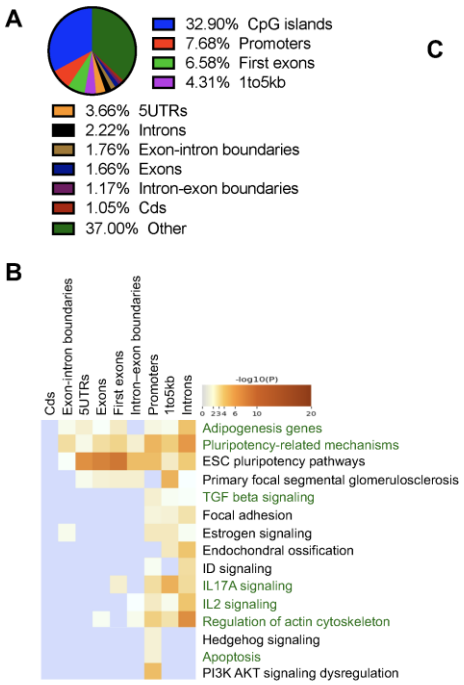

C

Enriched pathway	List of genes
Adipogenesis genes	Plin2,Ahr,Bmp2,Ctnnb1,Celf1,Ddit3,E2f1,Ebf1,Egr2,Gata2,Gata4,Nr3c1,Hmga1,Lifr,Smad3,Mef2d,Ncoa2,Ppara,Rara,Rb1,Rbl1,Rxra,Rxrg,Ncor1,Scd1,Ncor2,Tgfb1,Tle3,Wnt5b,Mixl1,Foxo1,Mbnl1,Lpin2,Wwtr1,E2f4,Bmp3
Pluripotency related mechanisms	Acvr1,Akt1,Apc,Nr2f2,Bmpr2,Ctnnb1,Ccnd1,Cdh1,Crebbp,Ctbp1,Ctcf,Dazl,Cdk2ap1,Phc1,Smarcad1,Fgf5,Fgfr1,Grb2,Hand2,Igfbp3,Inhbb,Itgb1,Lifr,Lrp5,Lyar,Smad2,Smad3,Smad7,Mbd2,Mef2d,Nfkb1,Nodal,Pim1,Prkaca,Rbbp4,Rela,Rest,Rock2,Sin3a,Kdm5c,Sall3,Tbx3,Tcf7l1,Tfeb,Tert,Tgfb1,Tgfbr1,Trim24,Wnt3a,Yy1,Zic3,Mta2,Mapk1,Rif1,Niban1,Cad,Tfcp2l1,Nedd4l,Smarca5,Nkd1,Sall4,Kdm1a,Rcor2,Chd4,Raf1,Kdm6b,Pim3,Ipo9,Zfp281,Grsf1,Usp7,Smo,Ep300,Zscan10,Kmt2d
TGF beta signaling	Ctnnb1,Runx2,Crebbp,Fkbp1a,Jun,Smad2,Smad3,Smad6,Smad7,Nfkb1,Nog,Ski,Tgfb1,Tgfbr1,Tgif1,Mapk9,Zfp423,Ep300
IL17A signaling	Akt1,Bcl2,Hmgb1,Smad6,Smad7,Sqstm1,Pdgfa,Pdgfb,Ppp1r14b,Rela,Tgfb1,Serbp1,Psmc6,Arpc5,Mylk,Pik3c3
IL2 signaling	Akt1,Bcl2,Cbl,Crkl,Fyn,Gab2,Grb2,Nr3c1,Hsp90aa1,Kras,Mknk1,Nfkb1,Pik3ca,Pik3r1,Pik3r2,Plcb1,Rela,Tert,Ets1,Mapk1,Mapk14,Mapk8,Mapk9,Foxo3,Nmi,Raf1,Shb
Regulation of actin cytoskeleton	Actb,Apc,Bdkrb2,Csk,Fgd1,Fgf1,Fgf14,Fgf3,Fgf9,Fgfr1,Fgfr2,Mras,Pdgfa,Pdgfb,Pik3r1,Pip4k2a,Pxn,Vcl,Ezr,Mapk1,Arhgef7,Diaph3,Rras2,Pik3r4,Cyfip2,Mylk,Actn1,Raf1,Pak6,Mapk4,Arhgef4,Gsn,Pak5
Apoptosis	Akt1,Birc5,Bad,Bcl2,Bcl2l11,Bnip3l,Igf1r,Igf2,Ikbkb,Ikbkg,Irf2,Irf4,Jun,Mcl1,Nfkb1,Nfkbib,Pik3r1,Rela,Trp73,Map3k1,Irf5,Bok,Pmaip1

Figure 3. Hypermethylated genomic DNA in pigmented 3-mo *Abca4*$^{-/-}$ mice RPE. (A) Genomic distribution of DMCs in *Abca4*$^{-/-}$ versus wild-type RPE. (B) Gene ontology and pathway enrichment analysis of hypermethylated DMCs. (biological 3 samples, one RPE/EC per sample). (C) Hypermethylated gene list in key regulatory pathways affected in *Abca4*$^{-/-}$ mice RPE.

Table 3. month-old *Abca4*$^{-/-}$ mice on 129/Sv (Figure 3) and BALB/c (Figure 4) backgrounds, along with respective wild-type controls. In both models, the highest enrichment of DMCs was detected in proximal regulatory regions. DMCs were primarily located in CpG islands (32.90%), followed by promoters (7.68%), first exons (6.58%), and regions 1–5 kb upstream of genes (4.31%) in *Abca4*$^{-/-}$ pigmented mice (Figure 3A). Enrichment analysis revealed marked hypermethylation in pathways related to lipid synthesis (adipogenesis; *p*-value = 1.36×10^{-6}), key signaling pathway TGF-β (p-value = 1.31×10^{-5}), IL-17A (*p*-value = 6.73×10^{-6}), IL-2 (*p*-value = 5.27×10^{-8}), actin cytoskeleton regulation (p = 6.36×10^{-8}), maintenance of pluripotency (*p*-value = 2.44×10^{-11}), and apoptosis (*p*-value = 2.88×10^{-5}) (Figure 3B,C).

 doi:10.20944/preprints202509.0141.v1

Figure 4

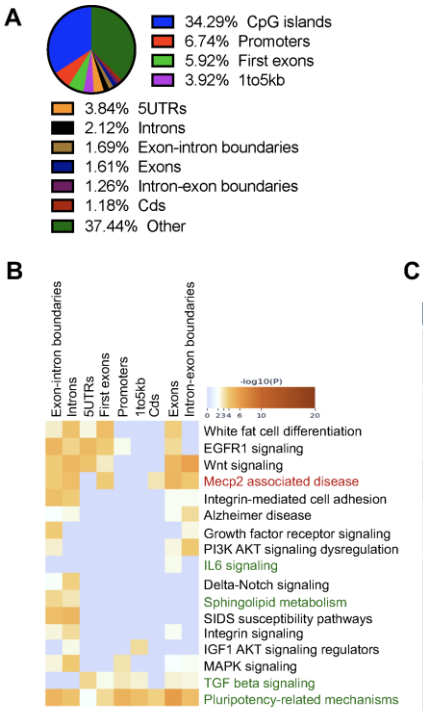

C

Enriched pathway	List of genes
Mecp2 and associated disease	Bcl6,Cebpd,Cnp,Creb1,Ctcf,Dlx5,E2f1,Fgf4,Gabrr2,Grin1,Nf1,Pou4f1,Rest,Sp3,Ybx1,Gprin1,Nrep,Fut8,Prpf3,Hnrnpf,Rbfox1
IL6 signaling	Akt1,Bad,Cdk5r1,Cebpb,Crebbp,Daxx,Erbb3,Ptk2,Fos,Fyn,Hras,Hspb1,Il6ra,Il6st,Jun,Ncoa1,Nfkb1,Nlk,Pik3r1,Ppp2ca,Ptk2b,Ptpn11,Pxn,Rb1,Sgk1,Map2k2,Map2k6,Mapk1,Mapk3,Foxo3
Sphingolipid metabolism	Degs1,Sgpl1,Sphk1,Sptlc2,Ugt8a,Sphk2,Kdsr,Cers2,Sgpp1,Sgms1,Cerk,Sptlc1
TGF beta signaling	Bmp4,Crebbp,Foxh1,Fkbp1a,Fos,Hras,Jun,Lef1,Smad1,Smad2,Smad3,Smad4,Smad7,Nfkb1,Tgfb1,Tgfbr1,Tgif1,Tnf,Mapk3,Zfp423
Pluripotency related mechanisms	Akt1,Axin1,Bmp4,Klf5,Cdh1,Creb1,Crebbp,Ctbp1,Ctbp2,Ctcf,Dazl,Ddb1,Dnmt1,Fgf4,Fgf5,Fos,Fzd1,Hells,Foxd3,Hira,Hras,Igfbp3,Il6st,Inhbb,Klf2,Lef1,Lrp5,Smad1,Smad2,Smad3,Smad4,Smad7,Mybl2,Ncoa1,Nfkb1,Nme2,Uhrf1,Npr1,Prkaca,Pml,Psen1,Ptpn11,Ptprs,Rel,Rest,Rock2,Sgk1,Sox2,Sp3,Sall3,Tcf7l1,Tfap2c,Terf2,Tgfb1,Tgfbr1,Nr2c1,Wnt3a,Sf1,Zic2,Mta2,Mapk1,Mapk3,Hnrnpu,Suz12,Smarca2,Cad,Zfp219,Stk40,Cers2,Nedd4l,Trim33,Sall4,Etv5,Cabin1,Chd4,Pim3,Zfp281,Ipo7,Smo,Kmt2d

Figure 4. Hypermethylated genomic DNA in albino 3-mo *Abca4*$^{-/-}$ mice RPE. (A) Genomic distribution of DMCs in *Abca4*$^{-/-}$ versus wild-type RPE. (B) Gene ontology and pathway enrichment analysis of hypermethylated DMCs. (biological 3 samples, one RPE/EC per sample). (C) Hypermethylated gene list in key regulatory pathways affected in *Abca4*$^{-/-}$ mice RPE.

In the RPE of 3-month-old *Abca4*$^{-/-}$ mice on BALB/c albino background, 34.29% of DMCs were located within CpG islands, followed by 6.74% in promoter regions, 5.92% in first exons, and 3.92% in 1–5 kb upstream regions (Figure 4A). Hypermethylated genes were significantly enriched in pathways associated with MeCP2-related disorders (p-value = 2.1×10^{-8}), IL-6 signaling (p-value = 8.3×10^{-7}), TGF-β signaling (p-value = 8.7×10^{-7}), and pluripotency regulation (p-value = 3.8×10^{-13}) (Figure 4B,C), consistent with findings in 1-month and 3-month *Abca4*$^{-/-}$ RPE on 129/Sv background (Figure 1C and Figure 3B). Additionally, genes involved in sphingolipid metabolism, previously implicated in AMD pathogenesis [58], exhibited significant hypermethylation (p-value = 9.3×10^{-6}).

2.5. Age-Dependent Increase of MeCP2 Protein in Abca4$^{-/-}$ *Mice RPE and in Human RPE*

The observed deregulation of MeCP2-related genes prompted us to evaluate MeCP2 expression in RPE. Longitudinal immunoblot analysis revealed a striking ~2.5-fold increase in MeCP2 protein levels in *Abca4*$^{-/-}$ mouse RPE from 1 to ~6 months of age, compared to age-matched 129/Sv wild-type controls (Figure 5A,B). After 6 months, MeCP2 levels remained persistently elevated at ~2-fold above wild-type levels (Figure 5A,B). These results demonstrate a sustained, age-dependent dysregulation of MeCP2 in Abca4$^{-/-}$ RPE, implicating this epigenetic regulator as a potential driver of progressive RPE dysfunction. Supporting its translational relevance, analysis of publicly available data (GSE159435, PMID: 33934486) showed that MeCP2 transcript levels also increase with age in human RPE tissue (Figure 5C), suggesting a conserved age-associated role for MeCP2 in RPE homeostasis.

 doi:10.20944/preprints202509.0141.v1

Figure 5

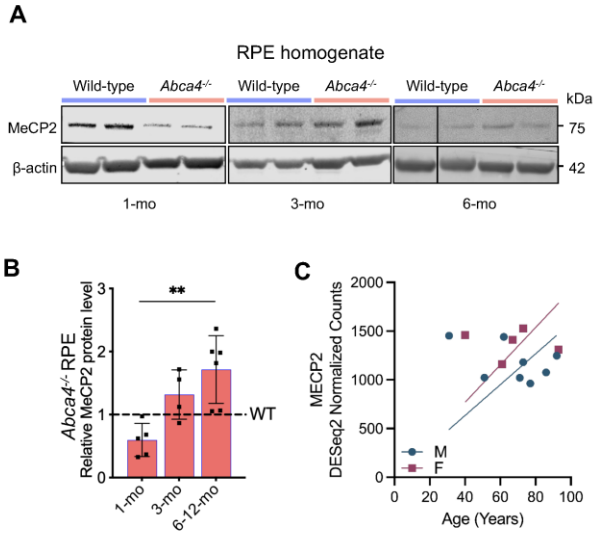

Figure 5. Age-dependent increase of MeCP2 protein in pigmented *Abca4*$^{-/-}$ mice RPE and human MeCP2 data. (A) Representative immunoblots for MeCP2 and *β*-actin as internal control in 1-mo,3-mo and 6-month-old *Abca4*$^{-/-}$ and wild-type mice RPE/eyecup (30µg total protein/lane). (B) Level of MeCP2 protein normalized to *β*-actin is plotted relative to wild-type (WT) levels, with 6-mo and 12-mo sample data combined. Experiment was repeated twice (single RPE/eyecup per sample, 5-6 mice/genotype). Data is represented as mean ± SD. adjusted $^{**}p < 0.01$; Two-way ANOVA with Bonferroni correction. (C) MeCP2 protein levels in human (male-M, female-F) RPE with aging.

3. Discussion

This study serves as a *proof-of-concept* that epigenetic dysregulation, mediated by altered DNA methylation and MeCP2-REST signaling, contributes to early RPE pathology and highlights the need to understand how epigenetic factors, alongside *ABCA4* genetic mutations, influence disease progression and severity in Stargardt patients. STGD1 is a highly heterogeneous macular dystrophy in terms of age of onset, disease progression, and clinical presentations. The genetic and phenotypic variability poses challenges for diagnosis and treatment, and cell-specific pathophysiological processes responsible for ABCA4-mediated maculopathies are still understudied.

DNA methylation changes are increasingly recognized as key epigenetic modifications involved in the pathogenesis of AMD, a related disease manifesting with RPE degeneration [60–62]. Multiple studies demonstrate altered DNA methylation patterns in RPE and peripheral blood of AMD patients, including hypomethylation of genes such as IL17RC, which leads to increased expression, and are linked to AMD progression [63,64]. Genome-wide methylation profiling reveals numerous differentially methylated regions in AMD samples, affecting genes that regulate oxidative stress responses, inflammation, and metabolic pathways [65–67]. This epigenetic dysregulation can modulate gene expression crucial for RPE cell function and survival, contributing to retinal degeneration, highlighting the dynamic interplay between genetics, environment, and epigenetics in initiating the pathology and disease progression [65,68–72]. To date, epigenetic regulation has not been studied on materials coming from STGD1 animal models or patient-derived RPE cells.

Here, we examined DNA methylation dynamics in the RPE of *Abca4*$^{-/-}$ mice and identified early, disease-relevant epigenetic changes that precede overt structural or functional decline. Although RPE integrity is preserved at 1 month of age, we observed differential DNA methylation in CpG islands, promoters, and first exons of key genes, implicating early epigenetic priming in disease initiation.

 doi:10.20944/preprints202509.0141.v1

These changes intensified by 3 months in two STGD1 mouse models, paralleling increased A2E-bisretinoid levels and autofluorescence [18,41,73,74], suggesting a progressive, methylation-mediated shift in RPE homeostasis. The pronounced changes in DNA methylation, predominantly at the proximal regulatory regions in *Abca4*$^{-/-}$ mice RPE, suggest a mechanism related to deregulation of gene transcription activation rather than mRNA splicing.

Many of the identified hypermethylated genes in *Abca4*$^{-/-}$ mice RPE are involved in pathways previously linked to aging and AMD, including cytokine signaling, cytoskeleton regulation, and cell metabolism [67,75]. For instance, hypermethylation of actin cytoskeleton-associated genes may impair RPE phagocytic capacity [76], while IL-6/IL-17A and TGF-β signaling pathways could exacerbate inflammation, fibrosis, and EMT, hallmarks of AMD [77], a disease clinically related to STGD1. Specifically, methylation changes in genes related to pluripotency and developmental regulation indicate possible dedifferentiation of *Abca4*$^{-/-}$ RPE cells and a higher probability of migration. These findings position DNA methylation as a potential driver of RPE dysfunction in STGD1, with relevance to other retinal diseases.

Transcriptomic analysis further supports this interpretation. In 1-month-old *Abca4*$^{-/-}$ RPE, gene expression changes were already evident in pathways regulating double-strand DNA repair, membrane potential, and inflammatory responses, indicating early, broader molecular dysregulation beyond bisretinoid toxicity caused by ABCA4 deficiency. Notably, our methylome-transcriptome analysis revealed enrichment for dysregulation of REST-mediated repression mechanisms, suggesting the role of MeCP2 in maintaining non-neuronal identity of RPE and showing an important epigenetic regulatory axis that is affected in diseased RPE. Interestingly, while dysregulation of inflammation and inflammation-related pathways could be detected on both transcriptional and epigenetic levels, several pathways differentially affected by hypermethylation in 1-month RPE were not deregulated at the transcriptional level at the same age. Precisely, hypermethylation was detected on genes involved in cell-cell adhesion and cytoskeleton remodeling, despite the absence of corresponding transcriptional or phenotypical changes. Notably, in STGD1, RPE cells undergo morphological and functional alterations driven by bisretinoid accumulation, oxidative stress, and complement dysregulation, which together disrupt cell adhesion and cytoskeleton integrity [11,18,78]. Emerging evidence from our study suggests that hypermethylation of genes governing these pathogenic pathways may represent an early step of disease-related changes in RPE, highlighting a potential epigenetic layer of gene regulation that amplifies the pathology.

We also found that MeCP2 protein levels progressively increased with age in *Abca4*$^{-/-}$ RPE, suggesting a role of MeCP2 in stabilizing hypermethylated chromatin and repressing transcription. Given MeCP2's ability to act as a context-dependent transcriptional regulator, it may exert wide-ranging effects on RPE gene networks. However, the overwhelming enrichment of DNA methylation changes in proximal regulatory regions suggests its key role in transcriptional repression. In addition, concurrent downregulation of genes with REST, a co-repressor often recruited by MeCP2, binding site at their promoters, suggests MeCP2-REST complex as a key component regulating transcriptional changes in the tissue. REST, known to silence neuronal genes in non-neuronal tissue [79–81], therefore plays a similar role in RPE [82]. However, it is also known to act as a transcription activator by recruiting TET3 hydroxylase and NSD3, a chromatin remodeler, to its promoters. Specifically, recruitment of TET3 to the REST-binding site causes conversion of methyl cytosine to 5-hydroxymethylcytosine, resulting in transcriptional activation [83]. In addition, REST-dependent recruitment of NSD3, a histone methyltransferase, promotes methylation of H3K36 residue, associated with active transcription [83]. With dynamic changes in DNA methylation patterns, and increasing levels of MeCP2 in the tissue, REST's role as a transcriptional repressor may shift to new promoter regions, including those normally associated with active gene expression in healthy tissue. Therefore, this potential of MeCP2 and REST's in establishing the transcriptional profile of diseased tissue adds a novel epigenetic dimension to the pathology of STGD1 and positions the MeCP2-REST complex as a candidate driver of age-related RPE functional decline.

 doi:10.20944/preprints202509.0141.v1

While our integrative approach offers valuable insights, several limitations must be acknowledged. First, our observations are primarily correlative, and the causal impact of the methylation changes on RPE dysfunction remains to be experimentally validated. Whether low-level bisretinoid accumulation (1-month) directly alters epigenetic regulators, or whether epigenetic dysregulation occurs independently in the *Abca4*$^{-/-}$ RPE, is still unknown. Second, although MeCP2 upregulation was observed, its genomic targets and co-factors, including REST, in RPE remain to be mapped, highlighting the need for MeCP2 chromatin immunoprecipitation sequencing (ChIP-seq) studies alongside age-stratified transcriptomic analysis. Third, the findings are currently limited to the RPE of the *Abca4*$^{-/-}$ STGD1 mouse model. Validation in human STGD1 RPE cells is essential to establish translational relevance. Lastly, while our study focuses on early stages (1-3 months), longitudinal profiling is necessary to understand how epigenetic regulation evolves throughout phenotype buildup to the stage that evidences RPE cell loss. Given the overlap in gene pathways between STGD1 and AMD, these findings also support the utility of the STGD1 models in studying age-related retinal degeneration more broadly.

In summary, our results reveal that DNA methylation changes and MeCP2-REST-mediated transcriptional repression occur before detectable RPE dysfunction in the STGD1 mouse model, suggesting they may play a role in disease progression. These findings not only provide a new understanding of epigenetic mechanisms in STGD1 but also highlight common molecular pathways with AMD. This work lays the groundwork for future investigations into epigenetic-based therapeutic strategies targeting RPE dysfunction in inherited and age-dependent macular diseases.

4. Materials and Methods

Mice

Abca4 null (*Abca4*$^{-/-}$) mice generated on two strains (129/Sv and BALB/c) were used in this study, as previously reported in [42,84]. Mice housed in normal cyclic 12-hour light/12-hour dark conditions were fed *ad libitum* with a standard rodent diet and were genotyped to confirm as negative for the Abca4 alleles. Sex distribution was kept the same in both the wild-type and *Abca4*$^{-/-}$ for experiments. All experiments followed the ARVO Statement for the Use of Animals in Ophthalmic and Vision Research and UCLA IACUC guidelines.

Collection of RPE/Eyecup

1- and 3-month 129/Sv strain and 3-month BALB/c mice were euthanized by cervical dislocation, and eyes from *Abca4*$^{-/-}$ and wild-type mice were harvested. In 1X phosphate buffer saline (PBS, pH 7.4), the anterior segment of the eye was removed, followed by the separation of the neural retina from the eyecup [9]. RPE/Eyecups were stored in a -80ºC freezer until further processing.

DNA Extraction and Quantification

DNA was extracted from mice, one RPE/eyecup per sample, using the Dneasy Blood & Tissue Kit (Qiagen, Cat# 69506). DNA was eluted in 50µl AE Buffer. The concentration was measured with the Qubit instrument (Life Technologies), and 100ng genomic DNA was treated with RNAse enzyme at 37ºC for 30 min to remove contaminating RNA.

Library Preparation and Reduced Representation Bisulphite Sequencing (RRBS)

RRBS libraries were prepared by Zymo-Seq RRBS Library kit (Cat# D5460). The libraries were subjected to size selection using magnetic AMPure XP beads (Beckman) to enrich DNA fragments of the desired size. The quality control of the final libraries (size-selected and barcoded) was performed using the Agilent TapStation 4200 (D1000, D5000). Pooled libraries were run on a NovaSeq 6000 as 100bp single-end reads.

 doi:10.20944/preprints202509.0141.v1

Data Analysis

Reads were aligned to the mm10 mouse reference genome using Bsbolt [85], followed by methylation calling using default parameters. Unsupervised and differential methylation analyses were conducted with RnBeads2 [86]. Briefly, sites were filtered based on coverage of 10 or more across 80% of the samples. Here, 653489 sites met the criteria. Methylation values were calculated as a value between 0 and 1, where 0 is not methylated and 1 is fully methylated. One sample was flagged as an outlier and removed from downstream analysis. Differential methylation analysis was performed using hierarchical linear models from the limma package and fitted using an empirical Bayes model [87] as implemented in the RnBeads2 package. Sites were considered differentially methylated if they reached an FDR-corrected significance level below 0.05 and a difference in the methylation value between the two groups of at least 10%. Differentially methylated sites were then annotated using the annotatr package in R [88] and ChipSeeker [89], with enrichment analysis performed using clusterProfiler [90] and Metascape [91] with the mouse reference genome as a background.

RNA Sequencing Data Set Enrichment Analysis

The RNA-seq dataset- list of the differentially expressed genes was acquired from NCBI (https://www.ncbi.nlm.nih.gov/bioproject/PRJNA269047) [92]. Upregulated and downregulated expressed genes in *Abca4*$^{-/-}$ versus wild-type were sorted based on the log2(fold change) and significance level $p<0.05$. Gene pathway enrichment analysis was performed using Metascape software [91] with the mouse reference genome as a background.

Immunoblotting

RPE/Eyecups from 1-, 3-, 6-, and 12-month-old *Abca4*$^{-/-}$ and age-gender matched 129/Sv wild-type mice were collected in 1X PBS with 1X Halt protease inhibitor cocktail (Thermo Scientific, Cat# 78429). Tissues were lysed by sonicating for 20 seconds. Tissue lysates were incubated with 1X Benzonase nuclease (EMD Millipore, Cat# 71205-3) for 1 hour, followed by 20 minutes of 0.5% SDS (Sigma-Aldrich, Cat# L3771) with gentle agitation at room temperature. Separation of Protein lysates from cell debris was achieved by spinning at 3,000x rpm for 5 minutes at 4°C. Total protein was estimated using Micro BCA Protein Assay Kit (Thermo Scientific, Cat# 23235). 40 µg of total protein was separated on 12% Bis-Tris polyacrylamide gels (Thermo Scientific, Cat# NP0341BOX) by running in 1X MOPS buffer at 100V. Proteins were transferred to PVDF membrane (EMD Millipore, Cat# IPFL00010) in 1X transfer buffer (Thermo Scientific, Cat# NP00061) using semi-dry transfer cell (Bio-rad) for 45 minutes at 20V. Membrane was blocked with protein-free Blocking Buffer (LI-COR Biosciences, Cat# 927-90010) at RT for 1 hour on a rocker and probed with MeCP2 (Cell Signaling Technology, Cat# 3456S) or (Abcam, Cat# ab2829) (1:1,000 dilution) and β-actin (Thermo Scientific, Cat# MA5-15452) (1:1000 dilution) primary antibodies in blocking buffer with 0.5% donkey serum overnight on rocker at 4°C. Membrane was washed with 1X PBS-T (0.1% Tween 20) 3 times for 5 minutes. LI-COR IRDye-680 or -800 channel secondary antibody (1:10,000 dilution) in blocking buffer with 0.5% donkey serum, incubation for 1 hour at RT on rocker was done, followed by a washing step 3 times for 5 minutes on a rocker. Membrane bands were imaged using the Odyssey CLx Infrared Imaging System and software (LI-COR). Band intensities were quantified with Image Studio Lite Ver 5.2. Statistical analysis was performed using GraphPad Prism 9.

Author Contributions: AD , DSK, and RAR conceptualized the manuscript; MM, AD, and RAR performed experiments; AD, AT, DSK, ET, and RAR analyzed data; AT, AD, ET, and DSK generated the figures and illustrations; AD wrote the original draft under guidance of DSK and RAR; all authors reviewed, revised, and approved the final draft; MP and RAR provided collaboration and funding support, respectively, to complete study.

Funding: The study was supported by the National Eye Institute grants R01 EY025002 (RAR) and P30-EY000331 Jules Stein Eye Institute Core Grant for Vision Research, unrestricted grant from Research to Prevent Blindness,

 doi:10.20944/preprints202509.0141.v1

Inc. (RPB, New York), Patricia and Joseph Yzurdiaga Vision Research Fund (RAR); and the Daljit S. and Elaine Sarkaria Charitable Foundation (RAR). R.A.R. holds the Vernon O. Underwood Family Endowed Chair in Ophthalmology, UCLA David Geffen School of Medicine.

Data Availability Statement: The data generated and analyzed during the current study will be available upon request to radu@jsei.ucla.edu (Roxana Radu) or arpita2269@g.ucla.edu (Arpita Dave). Sequencing data have been deposited in [repository XXX] under the accession number [XXXX].

Acknowledgments: We want to thank Eudia Sze Rou Ng and Saketh Dasarathi for their support with formatting and data analysis, respectively, as well as Zhichun Jiang and Simran Purohit for their assistance with animal work.

Conflicts of Interest: The authors declare no competing interests in the current study.

Abbreviations

The following abbreviations are used in this manuscript:

STGD1	Recessive Stargardt disease
AMD	Age-related macular degeneration
RRBS	Reduced Representation Bisulfite Sequencing
DMC	Differentially methylated CpGs

References

1. Strauss, R.W., et al., *The natural history of the progression of atrophy secondary to Stargardt disease (ProgStar) studies: design and baseline characteristics: ProgStar Report No. 1.* Ophthalmology, 2016. **123**(4): p. 817-828.
2. Lindner, M., et al., *Differential disease progression in atrophic age-related macular degeneration and late-onset Stargardt disease.* Investigative Ophthalmology & Visual Science, 2017. **58**(2): p. 1001-1007.
3. Cideciyan, A.V., et al., *Mutations in ABCA4 result in accumulation of lipofuscin before slowing of the retinoid cycle: a reappraisal of the human disease sequence.* Human molecular genetics, 2004. **13**(5): p. 525-534.
4. Alabduljalil, T., et al., *Correlation of outer retinal degeneration and choriocapillaris loss in Stargardt disease using en face optical coherence tomography and optical coherence tomography angiography.* American journal of ophthalmology, 2019. **202**: p. 79-90.
5. Allikmets, R., et al., *A photoreceptor cell-specific ATP-binding transporter gene (ABCR) is mutated in recessive Starqardt macular dystrophy.* Nature genetics, 1997. **15**(3): p. 236-246.
6. NCBI, *ClinVar search results for ABCA4 gene in Stargardt disease.* National Center for Biotechnology Information, n.d.
7. Sun, H. and J. Nathans, *Stargardt's ABCR is localized to the disc membrane of retinal rod outer segments.* Nature genetics, 1997. **17**(1): p. 15-16.
8. Illing, M., L.L. Molday, and R.S. Molday, *The 220-kDa rim protein of retinal rod outer segments is a member of the ABC transporter superfamily.* Journal of Biological Chemistry, 1997. **272**(15): p. 10303-10310.
9. Lenis, T.L., et al., *Expression of ABCA4 in the retinal pigment epithelium and its implications for Stargardt macular degeneration.* Proceedings of the National Academy of Sciences, 2018. **115**(47): p. E11120-E11127.
10. Matynia, A., et al., *Assessing Variant Causality and Severity Using Retinal Pigment Epithelial Cells Derived from Stargardt Disease Patients.* Translational vision science & technology, 2022. **11**(3): p. 33-33.
11. Ng, E.S.Y., et al., *Membrane Attack Complex Mediates Retinal Pigment Epithelium Cell Death in Stargardt Macular Degeneration.* Cells, 2022. **11**(21): p. 3462.
12. Farnoodian, M., et al., *Cell-autonomous lipid-handling defects in Stargardt iPSC-derived retinal pigment epithelium cells.* Stem Cell Reports, 2022. **17**(11): p. 2438-2450.
13. Molday, L.L., A.R. Rabin, and R.S. Molday, *ABCR expression in foveal cone photoreceptors and its role in Stargardt macular dystrophy.* Nature genetics, 2000. **25**(3): p. 257-258.
14. Mata, N.L., J. Weng, and G.H. Travis, *Biosynthesis of a major lipofuscin fluorophore in mice and humans with ABCR-mediated retinal and macular degeneration.* Proceedings of the National Academy of Sciences, 2000. **97**(13): p. 7154-7159.

 doi:10.20944/preprints202509.0141.v1

15. Weng, J., et al., *Insights into the function of Rim protein in photoreceptors and etiology of Stargardt's disease from the phenotype in abcr knockout mice.* Cell, 1999. **98**(1): p. 13-23.
16. Zhao, J., et al., *A vicious cycle of bisretinoid formation and oxidation relevant to recessive Stargardt disease.* Journal of Biological Chemistry, 2021. **296**.
17. Ng, E.S.Y., et al., *Impaired cathepsin D in retinal pigment epithelium cells mediates Stargardt disease pathogenesis.* The FASEB Journal, 2024. **38**(11): p. e23720.
18. Radu, R.A., et al., *Complement system dysregulation and inflammation in the retinal pigment epithelium of a mouse model for Stargardt macular degeneration.* Journal of Biological Chemistry, 2011. **286**(21): p. 18593-18601.
19. Deaton, A.M. and A. Bird, *CpG islands and the regulation of transcription.* Genes & development, 2011. **25**(10): p. 1010-1022.
20. Bird, A. *Functions for DNA methylation in vertebrates*. in *Cold Spring Harbor Symposia on Quantitative Biology*. 1993. Cold Spring Harbor Laboratory Press.
21. Dhar, G.A., et al., *DNA methylation and regulation of gene expression: Guardian of our health.* The Nucleus, 2021. **64**(3): p. 259-270.
22. Moore, L.D., T. Le, and G. Fan, *DNA methylation and its basic function.* Neuropsychopharmacology, 2013. **38**(1): p. 23-38.
23. Corso-Díaz, X., et al., *Epigenetic control of gene regulation during development and disease: A view from the retina.* Progress in retinal and eye research, 2018. **65**: p. 1-27.
24. Free, A., et al., *DNA recognition by the methyl-CpG binding domain of MeCP2.* Journal of Biological Chemistry, 2001. **276**(5): p. 3353-3360.
25. Amir, R.E., et al., *Rett syndrome is caused by mutations in X-linked MECP2, encoding methyl-CpG-binding protein 2.* Nature genetics, 1999. **23**(2): p. 185-188.
26. Meehan, R., J.D. Lewis, and A.P. Bird, *Characterization of MeCP2, a vertebrate DNA binding protein with affinity for methylated DNA.* Nucleic acids research, 1992. **20**(19): p. 5085-5092.
27. Chahrour, M., et al., *MeCP2, a key contributor to neurological disease, activates and represses transcription.* Science, 2008. **320**(5880): p. 1224-1229.
28. Ben-Shachar, S., et al., *Mouse models of MeCP2 disorders share gene expression changes in the cerebellum and hypothalamus.* Human molecular genetics, 2009. **18**(13): p. 2431-2442.
29. Sharma, K., et al., *Involvement of MeCP2 in regulation of myelin-related gene expression in cultured rat oligodendrocytes.* Journal of molecular neuroscience, 2015. **57**: p. 176-184.
30. Cheng, T.-L., et al., *Regulation of mRNA splicing by MeCP2 via epigenetic modifications in the brain.* Scientific reports, 2017. **7**(1): p. 42790.
31. Fuks, F., et al., *The methyl-CpG-binding protein MeCP2 links DNA methylation to histone methylation.* Journal of Biological Chemistry, 2003. **278**(6): p. 4035-4040.
32. Collins, A.L., et al., *Mild overexpression of MeCP2 causes a progressive neurological disorder in mice.* Human molecular genetics, 2004. **13**(21): p. 2679-2689.
33. Mann, I., *The development of the human eye*. 1928: The University Press.
34. Song, C., et al., *DNA methylation reader MECP2: cell type-and differentiation stage-specific protein distribution.* Epigenetics & chromatin, 2014. **7**(1): p. 1-16.
35. Li, X., et al., *MeCP2-421-mediated RPE epithelial-mesenchymal transition and its relevance to the pathogenesis of proliferative vitreoretinopathy.* Journal of cellular and molecular medicine, 2020. **24**(16): p. 9420-9427.
36. Zhang, Y., et al., *Critical role of apoptosis in MeCP2-mediated epithelial–mesenchymal transition of ARPE-19 cells.* Journal of Cellular Physiology, 2024. **239**(12): p. e31429.
37. Zhao, X., et al., *MeCP2-Induced Alternations of Transcript Levels and m6A Methylation in Human Retinal Pigment Epithelium Cells.* ACS omega, 2023. **8**(50): p. 47964-47973.
38. Ghosh, S., et al., *A role for βA3/A1-crystallin in type 2 EMT of RPE cells occurring in dry age-related macular degeneration.* Investigative ophthalmology & visual science, 2018. **59**(4): p. AMD104-AMD113.
39. Frasca, A., et al., *MECP2 mutations affect ciliogenesis: a novel perspective for Rett syndrome and related disorders.* EMBO Molecular Medicine, 2020. **12**(6): p. e10270.
40. Sun, C., J. Zhou, and X. Meng, *Primary cilia in retinal pigment epithelium development and diseases.* Journal of Cellular and Molecular Medicine, 2021. **25**(19): p. 9084-9088.

 doi:10.20944/preprints202509.0141.v1

41. Issa, P.C., et al., *Fundus autofluorescence in the Abca4−/− mouse model of Stargardt disease—correlation with accumulation of A2E, retinal function, and histology.* Investigative ophthalmology & visual science, 2013. **54**(8): p. 5602-5612.
42. Radu, R.A., et al., *Accelerated accumulation of lipofuscin pigments in the RPE of a mouse model for ABCA4-mediated retinal dystrophies following Vitamin A supplementation.* Investigative ophthalmology & visual science, 2008. **49**(9): p. 3821-3829.
43. Wang, K., Siyu Liu, Laurie K. Svoboda, Christine A. Rygiel, Kari Neier, Tamara R. Jones, Justin A. Colacino, Dana C. Dolinoy, and Maureen A. Sartor., *Tissue-and sex-specific DNA methylation changes in mice perinatally exposed to lead (Pb).* Frontiers in genetics, 2020. **11: 840**.
44. Zhong, H. and X. Sun, *Contribution of interleukin-17A to retinal degenerative diseases.* Frontiers in Immunology, 2022. **13**: p. 847937.
45. Tesseur, I. and T. Wyss-Coray, *A role for TGF-β signaling in neurodegeneration: evidence from genetically engineered models.* Current Alzheimer Research, 2006. **3**(5): p. 505-513.
46. Marambaud, P., U. Dreses-Werringloer, and V. Vingtdeux, *Calcium signaling in neurodegeneration.* Molecular neurodegeneration, 2009. **4**(1): p. 20.
47. Gutiérrez-Vargas, J.A., et al., *Neurodegeneration and convergent factors contributing to the deterioration of the cytoskeleton in Alzheimer's disease, cerebral ischemia and multiple sclerosis.* Biomedical Reports, 2022. **16**(4): p. 27.
48. Lionaki, E., C. Ploumi, and N. Tavernarakis, *One-carbon metabolism: pulling the strings behind aging and neurodegeneration.* Cells, 2022. **11**(2): p. 214.
49. Pons-Espinal, M., et al., *Blocking IL-6 signaling prevents astrocyte-induced neurodegeneration in an iPSC-based model of Parkinson's disease.* JCI insight, 2024. **9**(3): p. e163359.
50. Keenan, A.B., et al., *ChEA3: transcription factor enrichment analysis by orthogonal omics integration.* Nucleic acids research, 2019. **47**(W1): p. W212-W224.
51. Tsutsui, H., et al., *The DNA-binding and transcriptional activities of MAZ, a myc-associated zinc finger protein, are regulated by casein kinase II.* Biochemical and biophysical research communications, 1999. **262**(1): p. 198-205.
52. Fry, C.J. and P.J. Farnham, *Context-dependent transcriptional regulation.* Journal of Biological Chemistry, 1999. **274**(42): p. 29583-29586.
53. Tsukada, J., et al., *The CCAAT/enhancer (C/EBP) family of basic-leucine zipper (bZIP) transcription factors is a multifaceted highly-regulated system for gene regulation.* Cytokine, 2011. **54**(1): p. 6-19.
54. Zheng, D., K. Zhao, and M.F. Mehler, *Profiling RE1/REST-mediated histone modifications in the human genome.* Genome biology, 2009. **10**(1): p. R9.
55. Song, Y., et al., *CTCF functions as an insulator for somatic genes and a chromatin remodeler for pluripotency genes during reprogramming.* Cell Reports, 2022. **39**(1).
56. Guida, N., et al., *Stroke causes DNA methylation at Ncx1 heart promoter in the brain via DNMT1/MeCP2/REST epigenetic complex.* Journal of the American Heart Association, 2024. **13**(6): p. e030460.
57. Ballas, N. and G. Mandel, *The many faces of REST oversee epigenetic programming of neuronal genes.* Current opinion in neurobiology, 2005. **15**(5): p. 500-506.
58. Álvarez-Barrios, A., et al., *Dysregulated lipid metabolism in a retinal pigment epithelial cell model and serum of patients with age-related macular degeneration.* BMC biology, 2025. **23**(1): p. 96.
59. Bassett, E.A. and V.A. Wallace, *Cell fate determination in the vertebrate retina.* Trends in neurosciences, 2012. **35**(9): p. 565-573.
60. Li, X., S. He, and M. Zhao, *An Updated Review of the Epigenetic Mechanism Underlying the Pathogenesis of Age-related Macular Degeneration.* Aging and disease, 2020. **11**(5): p. 1219.
61. Hamid, M.A., et al., *Anti-VEGF Drugs Influence Epigenetic Regulation and AMD-Specific Molecular Markers in ARPE-19 Cells.* Cells, 2021. **10**(4): p. 878.
62. Gemenetzi, M. and A. Lotery, *The role of epigenetics in age-related macular degeneration.* Eye, 2014. **28**(12): p. 1407-1417.
63. Shin, J.I. and J. Bayry, *A role for IL-17 in age-related macular degeneration.* Nature Reviews Immunology, 2013. **13**(9): p. 701-701.

 doi:10.20944/preprints202509.0141.v1

64. Wei, L., et al., *Hypomethylation of the IL17RC promoter associates with age-related macular degeneration.* Cell reports, 2012. **2**(5): p. 1151-1158.
65. Hunter, A., et al., *DNA methylation is associated with altered gene expression in AMD.* Investigative ophthalmology & visual science, 2012. **53**(4): p. 2089-2105.
66. Porter, L.F., et al., *Whole-genome methylation profiling of the retinal pigment epithelium of individuals with age-related macular degeneration reveals differential methylation of the SKI, GTF2H4, and TNXB genes.* Clinical epigenetics, 2019. **11**(1): p. 1-14.
67. Corso-Díaz, X., et al., *Genome-wide profiling identifies DNA methylation signatures of aging in rod photoreceptors associated with alterations in energy metabolism.* Cell reports, 2020. **31**(3).
68. Liu, Z., et al., *Integrated analysis of DNA methylation and RNA transcriptome during in vitro differentiation of human pluripotent stem cells into retinal pigment epithelial cells.* PLoS One, 2014. **9**(3): p. e91416.
69. Dvoriantchikova, G., R.J. Seemungal, and D. Ivanov, *The epigenetic basis for the impaired ability of adult murine retinal pigment epithelium cells to regenerate retinal tissue.* Scientific reports, 2019. **9**(1): p. 3860.
70. Jin, Z. and Y. Liu, *DNA methylation in human diseases.* Genes & diseases, 2018. **5**(1): p. 1-8.
71. Suuronen, T., et al., *Epigenetic regulation of clusterin/apolipoprotein J expression in retinal pigment epithelial cells.* Biochemical and biophysical research communications, 2007. **357**(2): p. 397-401.
72. Orozco, L.D., et al., *A systems biology approach uncovers novel disease mechanisms in age-related macular degeneration.* Cell Genomics, 2023. **3**(6).
73. Charbel Issa, P., et al., *Rescue of the Stargardt phenotype in Abca4 knockout mice through inhibition of vitamin A dimerization.* Proceedings of the National Academy of Sciences, 2015. **112**(27): p. 8415-8420.
74. Müller, P.L., et al., *Monoallelic ABCA4 mutations appear insufficient to cause retinopathy: a quantitative autofluorescence study.* Investigative ophthalmology & visual science, 2015. **56**(13): p. 8179-8186.
75. Gemenetzi, M. and A. Lotery, *Epigenetics in age-related macular degeneration: new discoveries and future perspectives.* Cellular and Molecular Life Sciences, 2020. **77**: p. 807-818.
76. Kwon, W., and S. A. Freeman *Phagocytosis by the Retinal Pigment Epithelium: Recognition, Resolution, Recycling.* Frontiers in Immunology, 2020. **11: 604205-604205**.
77. *Seven new loci associated with age-related macular degeneration.* Nature genetics, 2013. **45**(4): p. 433-439.
78. Hu, J., et al., *Evidence of complement dysregulation in outer retina of Stargardt disease donor eyes.* Redox biology, 2020. **37**: p. 101787.
79. Ballas, N., et al., *REST and its corepressors mediate plasticity of neuronal gene chromatin throughout neurogenesis.* Cell, 2005. **121**(4): p. 645-657.
80. Hall, A.M., et al., *NRSF–mediated repression of neuronal genes in developing brain persists in the absence of NRSF-Sin3 interaction.* bioRxiv, 2018: p. 245993.
81. Perera, A., et al., *TET3 is recruited by REST for context-specific hydroxymethylation and induction of gene expression.* Cell reports, 2015. **11**(2): p. 283-294.
82. Wang, Y., et al., *REST, regulated by RA through miR-29a and the proteasome pathway, plays a crucial role in RPC proliferation and differentiation.* Cell Death & Disease, 2018. **9**(5): p. 444.
83. Perera A, E.D., Wagner M, Laube SK, Künzel AF, Koch S, Steinbacher J, Schulze E, Splith V, Mittermeier N, Müller M, *TET3 is recruited by REST for context-specific hydroxymethylation and induction of gene expression.* Cell reports, 2015. **11, no. 2: 283-294.**
84. Radu, R.A., et al., *Light exposure stimulates formation of A2E oxiranes in a mouse model of Stargardt's macular degeneration.* Proceedings of the National Academy of Sciences, 2004. **101**(16): p. 5928-5933.
85. Farrell, C., et al., *BiSulfite Bolt: A bisulfite sequencing analysis platform.* GigaScience, 2021. **10**(5): p. giab033.
86. Müller, F., et al., *RnBeads 2.0: comprehensive analysis of DNA methylation data.* Genome biology, 2019. **20**: p. 1-12.
87. Ritchie, M.E., et al., *limma powers differential expression analyses for RNA-sequencing and microarray studies.* Nucleic acids research, 2015. **43**(7): p. e47-e47.
88. Cavalcante, R.G. and M.A. Sartor, *Annotatr: genomic regions in context.* Bioinformatics, 2017. **33**(15): p. 2381-2383.
89. Wang, Q., et al., *Exploring epigenomic datasets by ChIPseeker.* Current protocols, 2022. **2**(10): p. e585.
90. Xu, S., et al., *Using clusterProfiler to characterize multiomics data.* Nature protocols, 2024. **19**(11): p. 3292-3320.

 doi:10.20944/preprints202509.0141.v1

91. Zhou, Y., et al., *Metascape provides a biologist-oriented resource for the analysis of systems-level datasets.* Nature communications, 2019. **10**(1): p. 1523.
92. Zhang, N., et al., *Protein misfolding and the pathogenesis of ABCA4-associated retinal degenerations.* Human molecular genetics, 2015. **24**(11): p. 3220-3237.